Large vortex-like structure of dipole field in computer models of liquid water and dipole-bridge between biomolecules

Junichi Higo*†‡, Masaki Sasai†§, Hiroki Shirai¶‖, Haruki Nakamura, and Takaki Kugimiya§**

*Biomolecular Engineering Research Institute (BERI), 6-2-3, Furuedai, Suita, Osaka 565-0874, Japan; §Graduate School of Human Informatics, Nagoya University, Nagoya 464-8601, Japan; ¶Tanabe Seiyaku, Kashima, Yodogawa, Osaka 532-8505 Japan; and **Institute for Protein Research, Osaka University, 3-2 Yamadaoka, Suita, Osaka 565-0871, Japan

Edited by Hans Frauenfelder, Los Alamos National Laboratory, Los Alamos, NM, and approved March 15, 2001 (received for review October 30, 2000)

We propose a framework to describe the cooperative orientational motions of water molecules in liquid water and around solute molecules in water solutions. From molecular dynamics (MD) simulation a new quantity ''site-dipole field'' is defined as the averaged orientation of water molecules that pass through each spatial position. In the site-dipole field of bulk water we found large vortex-like structures of more than 10 Å in size. Such coherent patterns persist more than 300 ps although the orientational memory of individual molecules is quickly lost. A 1-ns MD simulation of systems consisting of two amino acids shows that the fluctuations of site-dipole field of solvent are pinned around the amino acids, resulting in a stable dipole-bridge between side-chains of amino acids. The dipole-bridge is significantly formed even for the side-chain separation of 14 Å, which corresponds to five layers of water. The way that dipole-bridge forms sensitively depends on the side-chain orientations and thereby explains the specificity in the solvent-mediated interactions between biomolecules.

In order to understand the dynamics of solute molecules and biomolecule functioning in water solution, it should be a key issue to properly describe the cooperative motions of solvent water molecules. Although the molecular dynamics (MD) analyses have been devoted to finding the statistical laws of motions of water molecules (1) and the collective hierarchical features of dynamics in the hydrogen-bond network rearrangement have been found (2, 3), a clear theoretical picture of these complex motions has not yet been obtained.

Those who study structure and dynamics of the liquid state should be often confronted with the observations that molecules have two faces: In one observation molecules move cooperatively or collectively and in the other observation each molecule moves strongly randomly and chaotically. Cooperativity of motions of water molecules is manifested in the observed correlation between orientations of neighboring molecules (4). Each molecule, on the other hand, rapidly translates and rotates with a 5–10-ps time scale (1, 4), leading to quick randomization of orientations. Here, we propose a framework to describe these two faces of water molecules in a unified way by introducing a new quantity, site-dipole field. The site dipole is defined at each spatial position by the averaged orientation of water molecules that pass through that position. Although each water molecule randomly moves and quickly passes through each spatial site, we may expect that the coherent pattern remains in the site-dipole field because of the cooperativity among water molecules. Such coherent patterns in the bulk water should be perturbed by the presence of solute molecules to give rise to a characteristic site-dipole structure around the solute. We show that the coherent patterns indeed exist in the commonly used computer models of liquid water and that the structural ordering of site dipoles provides a perspective to understand hydration of biomolecules.

MD Simulations

Simulated Liquid Water. We performed three independent MD simulations of liquid water to examine how the features in the site-dipole field depend on the choice of potential and boundary condition. We used the most commonly studied water potential function, SPC/E (5) or TIP3P (6). (*i*) 1,000 water molecules of the SPC/E potential were simulated under the microcanonical condition in a periodic box with density 0.997 g/cm^3 at the average temperature 298 K. The side length of the box is L_{box} = 31.065 Å. The Coulomb interaction was treated by the reaction-field method (7) with the radius of $L_{box}/2$ for the direct sum. (*ii*) 216 SPC/E water molecules were computed in a periodic box under the canonical condition (298 K) with the Ewald method for the Coulomb interaction. (*iii*) 6,075 TIP3P water molecules were confined in a sphere (diameter = 70 Å) under the canonical condition (300 K). A cell-multipole expansion method (8) was used for the Coulomb interaction. All three simulations were done for 300 ps, after a 100-ps equilibrium run with a time step of 1 fs and with snapshots sampled every 10 fs, and gave qualitatively identical results for the existence of vortices in dipole-field. In the following sections, the results from simulation (*i*) are explained, if it is not clearly mentioned which simulation is focused on. The 300-ps sampling run and 100-ps equilibrium run were long enough to analyze the collective features of the site-dipoles (9, 10). We also performed a 1-ns MD simulation of a protein and found that a site-dipole field around the protein calculated from a subtrajectory of 300 ps, which was extracted from a 1-ns trajectory, was qualitatively similar to the field from the full trajectory of 1ns (J.H. and M. Nakasako, unpublished work).

Three Systems of Amino Acids. In a system consisting of large biomolecules, a number of charged and polar groups contribute to the interaction between the biomolecules. Here, we introduce three simple systems of amino acids to analyze the essential factors for the biomolecular interaction. Each system consists of two amino acids, Ace-Asp-Nme and Ace-Arg-Nme, where Ace and Nme are the N-terminal acetyl and C-terminal *N*-methyl groups, respectively, to reduce the effect of charge at the termini of amino acids. Amino acids Asp and Arg are negatively and positively charged, respectively, and frequently found on the protein surface. All dihedral angles in the amino acids are set to 180°, where the side-chain conformations are extended. This is to mimic a situation that the side-chains on the protein surface are highly exposed in solution.

This paper was submitted directly (Track II) to the PNAS office.

Abbreviation: MD, molecular dynamics.

†To whom reprint requests should be addressed. E-mail: higo@ls.toyaku.ac.jp or sasai@info.human,nagoya-u.ac.jp.

‡Present address: Laboratory of Bioinformatics, School of Life Science, University of Pharmacy and Life Science, 1432-1 Horinouchi, Hachioji, Tokyo 192-0392, Japan.

‖Present address: Department of Biochemistry, University of Cambridge, 80 Tennis Court Road, Old Addenbrookes Site, Cambridge CB2 1GA, United Kingdom.

The publication costs of this article were defrayed in part by page charge payment. This article must therefore be hereby marked "*advertisement*" in accordance with 18 U.S.C. §1734 solely to indicate this fact.

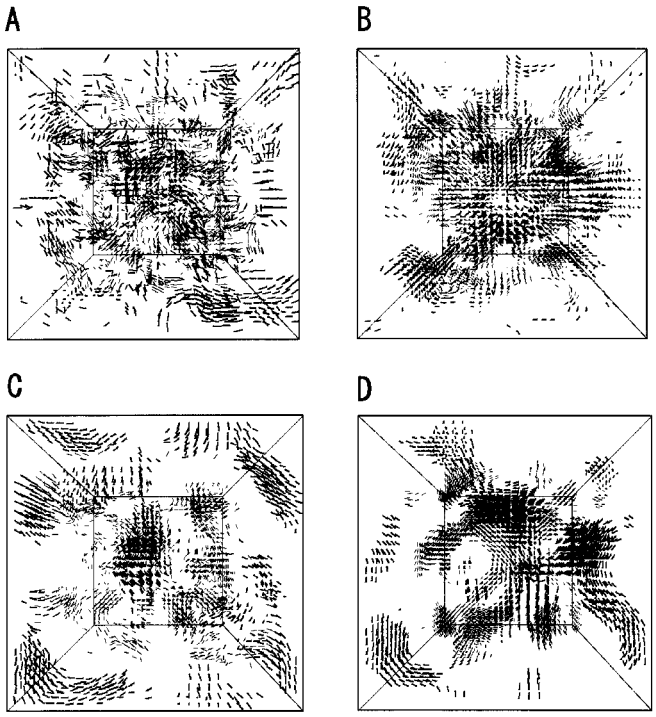

Fig. 1. Typical patterns of the coarse-grained site dipoles and vorticities found in the MD simulation (*i*). (*A*) Instantaneous site dipoles, $\bar{\mathbf{d}}(\mathbf{r}_i,R,t)$, coarse grained with sphere of $R = 3L_{\text{cube}}$ at an exemplified instance *t*. Vectors with length $|\bar{\mathbf{d}}| \geq 0.8 \times |\bar{\mathbf{d}}_{\max}|$ are shown by bars. (*B*) Time-averaged site dipoles over the duration $w = 300$ ps, $\bar{\mathbf{d}}_w(\mathbf{r}_i,R)$, coarse grained with $R = 2L_{\text{cube}}$. Vectors with length $|\bar{\mathbf{d}}_w| \geq 0.45 \times |\bar{\mathbf{d}}_{w,\max}|$ are shown by bars. (*C*) Vorticity of the instantaneous site dipoles, $\mathbf{v}(\mathbf{r}_i,R,t)$, calculated with the sphere of $R = 6L_{\text{cube}}$ at the same instance *t* as in *A*. Vectors with length $|\mathbf{v}| \geq 0.6 \times |\mathbf{v}_{\max}|$ are shown by bars. (*D*) Vorticity of the time-averaged site dipoles over 300 ps, $\mathbf{v}_w(\mathbf{r}_i,R)$, calculated with $R = 6L_{\text{cube}}$. Vectors with length $|\mathbf{v}_w| \geq 0.55 \times |\mathbf{v}_{w,\max}|$ are shown by bars.

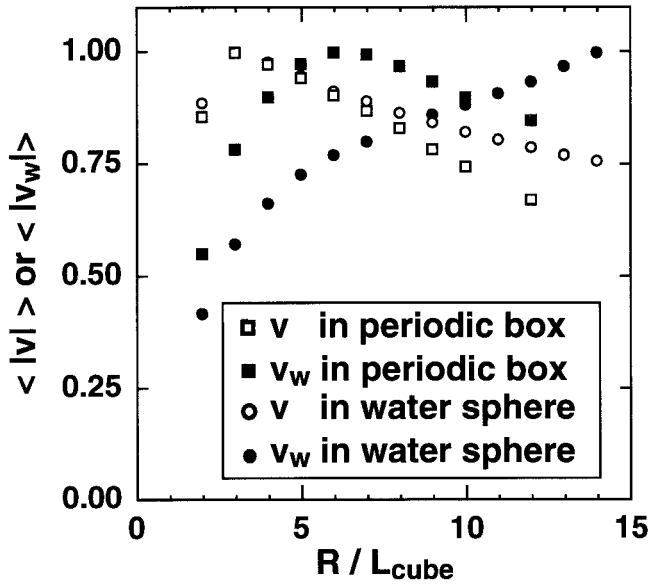

Fig. 2. *R*-dependence of the mean amplitude of the instant and time-averaged vorticities, $\langle|\mathbf{v}(\mathbf{r}_i,R,t)|\rangle$ and $\langle|\mathbf{v}_w(\mathbf{r}_i,R)|\rangle$ ($w = 300$ ps), where $\langle \ldots \rangle$ represents average over $\mathbf{r}_i$. Values are normalized by their maxima. See *MD Simulations* for the simulations in the periodic box (1,000 water molecules) and in water sphere.

The tip of the side-chain forms a triangle of three heavy atoms: {CG, OD1, OD2} for Asp, {CZ, NH1, NH2} for Arg. The two triangles are put on a plane with distance settings for OD1-NH1 and OD2-NH2 of 8 Å for system A or to 14 Å for system C. System B is generated from system A, with rotation of Arg by 90° around the vector pointing from NH1 to NH2. Thus, the distances OD1-NH1 and OD2-NH2 are the same as those of system A (i.e., 8 Å). The amino acids are immersed in the sphere of TIP3P water (diameter = 50 Å), where the geometrical center of the two triangles are set to the center of the water sphere. The amino acid atoms are restrained by a harmonic function around the initial positions during the simulation (atomic displacements <0.2 Å). The cell-multipole expansion method was used. A 1-ns sampling was done at 300 K with a 1-fs time-step, after a high-temperature run (100 ps at 500 K) to break the hydrogen-bond network in the initial configuration and an equilibrium run (100 ps at 300 K). The MD program PRESTO (11) was used with an AMBER parm96 force field (12).

Vortices in Site-Dipole Field of Computed Liquid Water

In this section, we show that mesoscopic spatial patterns of molecular orientations exist not only in each MD snapshot, but also in the time-averaged orientations over the snapshots. Existence of the spatial patterns reflects collective features in the diffusive motions of water. Because of the rapid translations and rotations of individual molecules, quantities fixed on each moving water molecule do not clarify the collective features among molecules. Instead, we consider a site-dipole field defined on each fixed spatial position. The periodic box of the liquid-water system is divided into $30 \times 30 \times 30$ cubes with the side length $L_{\text{cube}} = L_{\text{box}}/30$. Then, $\mathbf{d}(\mathbf{r}_i,t)$ is introduced as the dipole moment of the *i*th cube at time *t* and is referred to as "site-dipole," where $\mathbf{r}_i$ is the body-center of the *i*th cube. The site-dipole $\mathbf{d}(\mathbf{r}_i,t)$, whose orientation is parallel to a vector pointing from the oxygen atom to the midpoint of two hydrogen atoms of a water molecule detected in the *i*th cube, is normalized as $|\mathbf{d}(\mathbf{r}_i,t)| = 1$, and $\mathbf{d}(\mathbf{r}_i,t) = 0$ when no water molecule is detected. We also introduce the time-averaged site-dipole $\mathbf{d}_w(\mathbf{r}_i)$, which is calculated by summing $\mathbf{d}(\mathbf{r}_i,t)$ over snapshots of the MD trajectory of a time length *w* and normalizing it by the number of times that molecules are detected in the *i*th cube during *w*.

The spatial patterns of the site-dipoles can be seen by coarse-graining $\mathbf{d}(\mathbf{r}_i,t)$ and $\mathbf{d}_w(\mathbf{r}_i)$ as $\bar{\mathbf{d}}(\mathbf{r}_i,R,t) = N_{\text{cube}}{}^{-1}\Sigma_j\, \mathbf{d}(\mathbf{r}_j,t)$ and $\bar{\mathbf{d}}_w(\mathbf{r}_i,R) = N_{\text{cube}}{}^{-1}\Sigma_j\, \mathbf{d}_w(\mathbf{r}_j)$, respectively. Here, $\mathbf{r}_i$ is the position vector of a cube in a sphere (radius = *R*) around the central cube at $\mathbf{r}_i$. The summation is taken over the in-sphere cubes and N_{cube} is the number of them. The coarse-grained quantities, $\bar{\mathbf{d}}(\mathbf{r}_i,R,t)$ and $\bar{\mathbf{d}}_w(\mathbf{r}_i,R)$, are exemplified in Fig. 1 *A* and *B*, respectively, where large winding patterns in the arrangement of site-dipoles are found. Then, we analyze these patterns by examining how the vectors, $\mathbf{d}(\mathbf{r}_j,t)$ or $\mathbf{d}_w(\mathbf{r}_j)$, "rotate" around the position $\mathbf{r}_i$. The "rotation" of the instant site-dipoles around $\mathbf{r}_i$ is defined as $\mathbf{v}(\mathbf{r}_i,R,t) = N_{\text{cube}}{}^{-1}\Sigma_j(\mathbf{r}_j - \mathbf{r}_i) \times \mathbf{d}(\mathbf{r}_j,t)$. Here, the orientation of $\mathbf{v}(\mathbf{r}_i,R,t)$ represents the rotation axis, around which $\mathbf{d}(\mathbf{r}_j,t)$ rotates, and the norm of $\mathbf{v}(\mathbf{r}_i,R,t)$ does the amount of rotation. Similarly, the rotation for the time-averaged site-dipoles is defined as $\mathbf{v}_w(\mathbf{r}_i,R) = N_{\text{cube}}{}^{-1}\Sigma_j(\mathbf{r}_j - \mathbf{r}_i) \times \mathbf{d}_w(\mathbf{r}_j)$. We call these vectors "volticities." Vortex structures in the instant site–dipole field, $\mathbf{v}(\mathbf{r}_i,R,t)$, and in the time-averaged site–dipole field, $\mathbf{v}_w(\mathbf{r}_i,R)$, are shown in Fig. 1 *C* and *D*, respectively. Fig. 1*D* shows that the large-scale coherent patterns survive after the time averaging over 300 ps.

Note that the existence of vortices is compatible to the known features of dipole relaxation: Random fluctuations of vortex shape should result in the short spatial correlation lengths and short relaxation times if they were measured by the two-body correlation functions. The rotational relaxation times of $\bar{\mathbf{d}}$ and $\mathbf{v}$

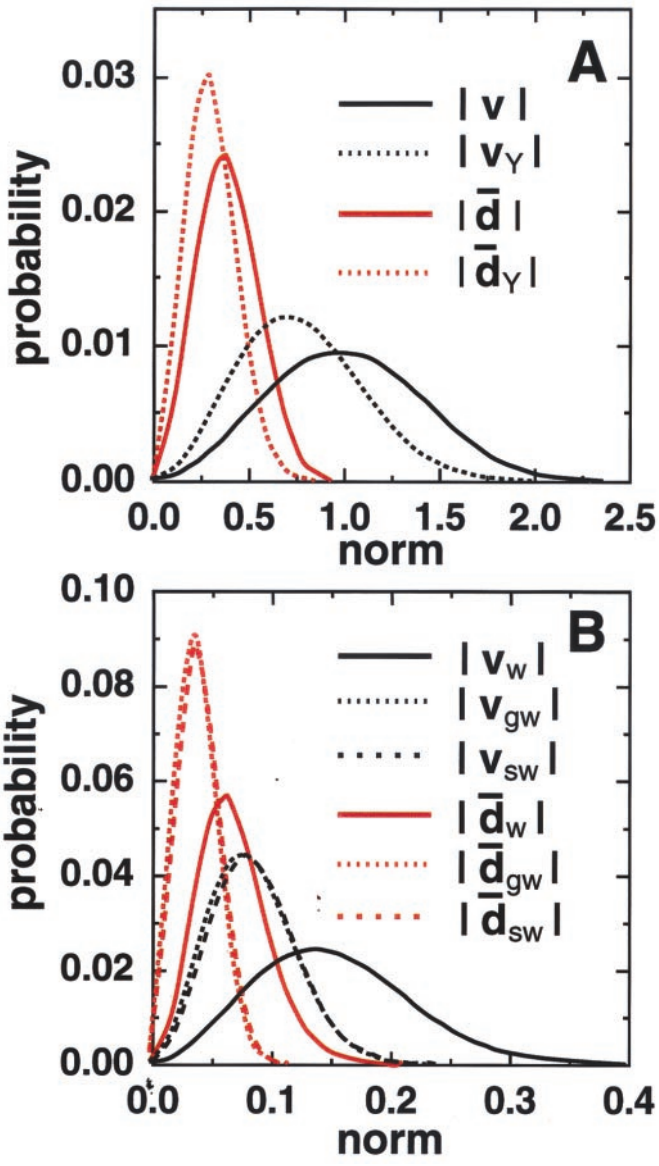

Fig. 3. Distributions of amplitude of the site dipoles in the MD model and in the noncorrelated model. The noncorrelated models were calculated by placing a randomly oriented unit vector $\mathbf{u}$ on each oxygen atom of moving water molecules along the MD trajectory. The orientations of $\mathbf{u}$ were changed by gradual or sudden rotation. In the gradual rotation, the orientation was renewed at each step of trajectory as $\mathbf{u} \rightarrow \mathbf{u}' = \mathbf{u} + \Delta\mathbf{u}$, where $\Delta\mathbf{u}$ was a small random vector and $\mathbf{u}'$ was normalized as $|\mathbf{u}'| = 1$. In the sudden rotation, $\mathbf{u}$ was randomly rotated at each step of trajectory with a small probability ε. The rotational relaxation time of $\mathbf{u}$ was set to the value ⟨5.2 ps⟩ in the current simulation in both rotations with modulating $\Delta\mathbf{u}$ or ε. (*A*) Distributions of amplitude of the coarse-grained site dipoles in the MD model, $|\bar{\mathbf{d}}(\mathbf{r}_i,R)|$, and in the noncorrelated model, $|\bar{\mathbf{d}}_Y(\mathbf{r}_i,R)|$, and distributions of amplitude of the vorticities in the MD model, $|\mathbf{v}(\mathbf{r}_i,R)|$, and in the noncorrelated model, $|\mathbf{v}_Y(\mathbf{r}_i,R)|$ ($R = 4L_{\text{cube}}$). Either gradual or sudden rotation provides exactly the same results. (*B*) Distributions of amplitude of the coarse-grained, time-averaged site dipoles in the MD model, $|\bar{\mathbf{d}}_w(\mathbf{r}_i,R)|$, and in the noncorrelated model, $|\bar{\mathbf{d}}_{Yw}(\mathbf{r}_i,R)|$, and distributions of amplitude of the time-averaged vorticities in the MD model, $|\mathbf{v}_w(\mathbf{r}_i,R)|$, and in the noncorrelated model, $|\mathbf{v}_{Yw}(\mathbf{r}_i,R)|$. Here, Y = ''g'' for the gradual rotation of the noncorrelated model and Y = ''s'' for the sudden rotation. w = 300 ps and $R = 4L_{\text{cube}}$.

for $R = 8L_{\text{cube}}$ were 6.5 ps and 6.9 ps, respectively. These are comparable to the single molecule relaxation time $\tau_s = 5.2$ ps in the present simulation. Spatial correlation lengths of $\mathbf{v}$ and $\mathbf{v}_w$

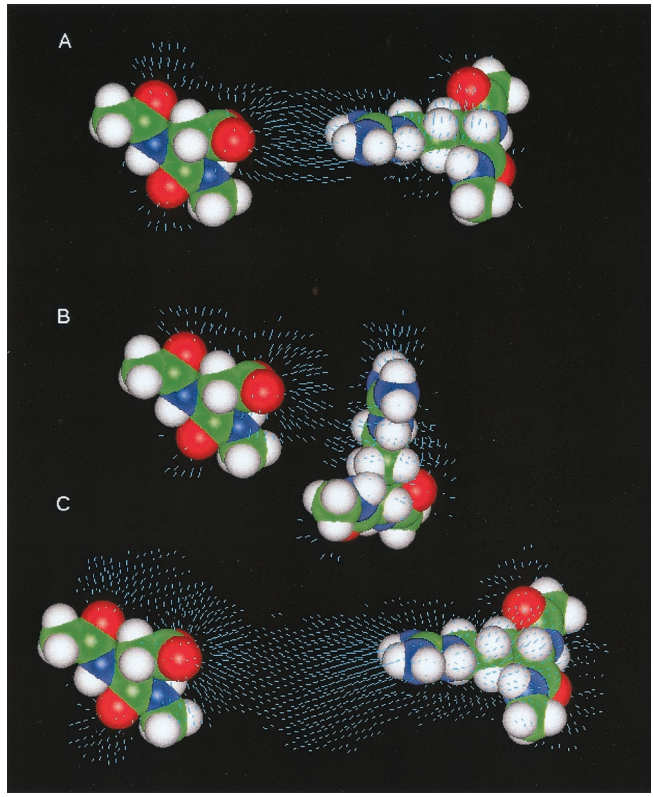

Fig. 4. Field of coarse-grained site-dipoles, $\bar{\mathbf{d}}_w(\mathbf{r}_i,R)$ (w = 1 ns and R = 2 Å), around amino acids. The site-dipole field was calculated by dividing space into 1 Å cubes. A bar represents the vector of $\bar{\mathbf{d}}_w(\mathbf{r}_i,R)$. (*A*) System A with $|\bar{\mathbf{d}}| \geq 0.4$, (*B*) system B with $|\bar{\mathbf{d}}| \geq 0.4$, and (*C*) system C with $|\bar{\mathbf{d}}| \geq 0.3$ (see *MD simulations* for definitions of systems A, B, and C).

were 3.2 Å, which extend to the distance between neighboring molecules.

The mesoscopic features of Fig. 1 become apparent in different statistics of the vorticities. In Fig. 2, R-dependence of norms of $\mathbf{v}(\mathbf{r}_i,R,t)$ and $\mathbf{v}_w(\mathbf{r}_i,R)$ are shown. The value $\langle|\mathbf{v}_w(\mathbf{r}_i,R)|\rangle$ has a maximum at $R = 6L_{\text{cube}}$, indicating that there exist large vortices of opposite directions with the size approximately half of the box (i.e., $2R \approx 12L_{\text{cube}} > 10$ Å to satisfy the periodic boundary condition of the box). The water-sphere simulation (*iii*), which is free from the periodicity of system, demonstrated that $\langle|\mathbf{v}_w(\mathbf{r}_i,R)|\rangle$ monotonically increases with R.

The statistical significance of the vorticity is assessed by using the noncorrelated model (see the caption for Fig. 3 for the definition), where the intermolecular orientations of dipoles were kept noncorrelated. The instantaneous and time-averaged site-dipoles were derived for the noncorrelated model, and the spatially coarse-grained dipoles, $\bar{\mathbf{d}}_Y(\mathbf{r}_i,R)$ and $\bar{\mathbf{d}}_{Yw}(\mathbf{r}_i,R)$, and vorticities, $\mathbf{v}_Y(\mathbf{r}_i,R)$ and $\mathbf{v}_{Yw}(\mathbf{r}_i,R)$, were calculated in the same manner as those for the site-dipoles in the original MD motions. Fig. 3*A* represents the distributions of the instantaneous quantities $|\bar{\mathbf{d}}(\mathbf{r}_i,R)|$, $|\bar{\mathbf{d}}_Y(\mathbf{r}_i,R)|$, $|\mathbf{v}(\mathbf{r}_i,R)|$, and $|\mathbf{v}_Y(\mathbf{r}_i,R)|$, and Fig. 3*B* represents those of the time-averaged quantities $|\bar{\mathbf{d}}_w(\mathbf{r}_i,R)|$, $|\bar{\mathbf{d}}_{Yw}(\mathbf{r}_i,R)|$, $|\mathbf{v}_w(\mathbf{r}_i,R)|$, and $|\mathbf{v}_{Yw}(\mathbf{r}_i,R)|$. The distributions of $|\bar{\mathbf{d}}(\mathbf{r}_i,R)|$ and $|\mathbf{v}(\mathbf{r}_i,R)|$ are shifted to the direction of larger R from the corresponding noncorrelated distributions of $|\bar{\mathbf{d}}_Y(\mathbf{r}_i,R)|$ and $|\mathbf{v}_Y(\mathbf{r}_i,R)|$, as shown in Fig. 3*A*. The shift is more evident in Fig. 3*B*. Thus, the existence of vortices in the MD data are statistically significant for both the instantaneous and time-averaged site-dipoles.

Dipole-Bridge Between Biomolecules

We found vortices of larger than 10 Å in size and of longer than 100 ps time-scale in the dipole field of simulated liquid water.

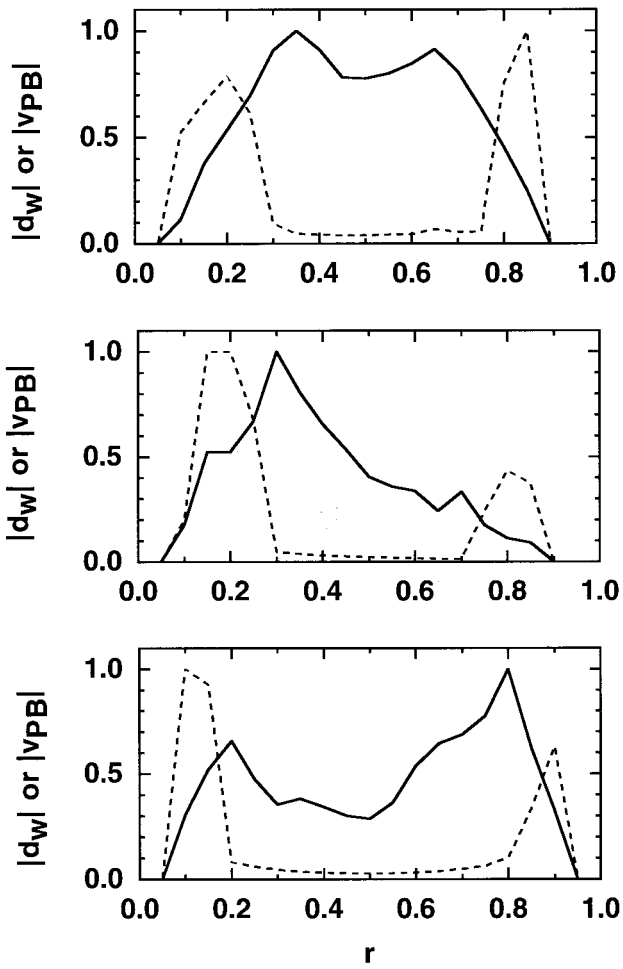

Fig. 5. Norm of time-averaged site-dipole, d_w (w = 1 ns), and Poisson–Boltzmann's electrostatic field, $\mathbf{v}_{PB}$, along the line between two side-chain tips. The line was drawn from the side-chain tip of Asp (average position of OD1 and OD2) to that of Arg (that of NH1 and NH2). (*A*) System A, (*B*) system B, and (*C*) system C. Solid lines are the norm of $\mathbf{d}_w$ and broken lines that of $\mathbf{v}_{PB}$. The *x* axis (r) is normalized by the distance between the side-chain tips (8 Å for system A and B, and 14 Å for system C) and the *y* axis is normalized by the largest norm along the line. The Poisson–Boltzmann equation was solved under the following condition: first, the two amino acids were put in a box ($50 \times 50 \times 50$ Å^3) so that the water sphere (diameter = 50 Å) was included in the box. Next, the box was divided into the 1 Å cubes in the same manner as the evaluation of the site-dipoles. Lastly, $\mathbf{v}_{PB}$ was calculated at each center of cubes. The dielectric constant was assumed to be 2.0 for cubes inside the amino acids, and 78.5 for those in the solvent region, where the Debye screening parameter was 0.0. The boundary of the box was calibrated by the self-consistent boundary method, by Green's function theorem (15), so that the electrostatic potential equals zero at infinity.

Universality of this mesoscopic structure of site-dipoles should be examined in a biological system. The MD simulations in the current work and refs. 11 and 12 demonstrated that the charge distribution and polarization in biomolecules enhance the ordering of site-dipoles in solvent. Fig. 4 *A* and *C* show that the site-dipole field forms a dipole-bridge between the amino acids, which persists over a time scale of 1 ns. Note that w = 1 ns is much longer than the rotational and translational diffusion times of water molecules. The existence of the dipole-bridge manifests that the orientation of a water molecule is statistically pinned by the site-dipole field when the water molecule is in the region of the dipole-bridge, although the orientation is quickly randomized when the water molecule leaves the dipole-bridge. Fig. 4*B* demonstrates that the side-chain orientation is important in forming the bridge. Analysis using the orientational distribution function defined by Cheng *et al.* (13, 14) showed that the clathrate-like structure of water is formed around the CG atom of Arg in system B (data not shown), which prevents the dipole-bridge from forming. Fig. 4*C* also shows that the formation of bridge is significant even for the side-chain separation of 14 Å, which corresponds to five layers of water. Because the dipole field makes the Kirkwood *G*-factor small, the dielectric constant becomes small in the bridge, which should result in the large enthalpic interaction between charged atoms of side-chains. We calculated the electrostatic field, $\mathbf{v}_{PB}$, from the Poisson–Boltzmann equation for these systems, and compared it with the site-dipole field. Fig. 5 shows the norm of the time-averaged site-dipole, $\mathbf{d}_w$ (w = 1 ns) and the norm of $\mathbf{v}_{PB}$, along the line between the two side-chain tips. Although $\mathbf{v}_{PB}$ is large near the side-chain atoms, it rapidly decays in the middle region of the two side-chains. This means that in any system, A, B, or C, $\mathbf{v}_{PB}$ does not provide a bridge of electrostatic field because of the screening effect of water. On the other hand, the norm of site-dipole is significantly large in the middle region and the dipole-bridge is formed in A and C. Fig. 5*B* shows that the norm of site-dipole field becomes smaller near the side-chain of Arg and that the dipole-bridge connection between two side chains in system B is much suppressed compared with system A. Thus, the site-dipole field method reveals a sensitive dependence of hydration on solute configuration, which cannot be found with the continuum Poisson–Boltzmann method. The finding of the mesoscopic structures in the dipole field should open a new view to understanding the hydration phenomena, and proposes a scheme in which the biomolecules may interact with each other through the dipole field.

We thank Drs. D. Koda and N. Ito from the Biomolecular Engineering Research Institute (BERI) for helpful discussions. This work was partially supported by Japan Science and Technology Cooperation and by Grants-in-aid from the Ministry of Education, Science, Sports and Culture, Japan.

1. Robinson, G. W., Zhu, S.-B., Singh, S. & Evans, M. W. (1996) *Water in Biology, Chemistry and Physics* (World Scientific, Singapore).
2. Ohmine, I. & Tanaka, H. (1993) *Chem. Rev. (Washington D.C.)* **93,** 2545–2566.
3. Starr, F. W., Harrington, S., Sciortino, F. & Stanley, H. E. (1999) *Phys. Rev. Lett.* **82,** 3629–3632.
4. Eisenberg, D. & Kauzman, W. (1969) *The Structures and Properties of Water* (Oxford Univ. Press, London).
5. Berendsen, H. J. C., Grigera, J. R. & Straatsma, T. P. (1987) *J. Phys. Chem.* **91,** 6269–6271.
6. Jorgensen, W. L., Chandrasekhar, J., Madura, J. D., Impey, R. W. & Klein, M. L. (1983) *J. Chem. Phys.* **79,** 926–935.
7. Steinhauser, O. (1982) *Mol. Phys.* **45,** 335–348.
8. Ding, H.-Q., Karasawa, N. & Goddard, W. A., III (1992) *J. Chem. Phys.* **97,** 4309–4315.
9. Higo, J., Kono, H., Nakajima, N., Shirai, H., Nakamura, H. & Sarai, A. (1999) *Chem. Phys. Lett.* **306,** 395–401.
10. Higo, J., Kono, H., Nakamura, H. & Sarai, A. (2000) *Proteins* **40,** 193–206.
11. Morikami, K., Nakai, T., Kidera, A., Saito, M. & Nakamura, H. (1992) *Comp. Chem.* **16,** 243–248.
12. Kollman, P., Dixson, R., Cornell, W., Fox, T., Chipot, C. & Pohorille, A. (1997) in *Computer Simulations of Biological Systems*, eds. Gunsteren, W. F., Weiner, P. K. & Wilkinson, A. J. (ESCOM, Dordrecht, The Netherlands), Vol. 3, pp. 83–94.
13. Cheng, Y.-K., Sheu, W.-S. & Roskky, P. J. (1999) *Biophys. J.* **76,** 1734–1743.
14. Cheng, Y.-K. & Roskky, P. J. (1998) *Nature (London)* **392,** 696–699.
15. Nakamura, H. (1996) *Q. Rev. Biophys.* **29,** 1–90.